ENVIRONMENTAL RESEARCH
CLIMATE

PAPER • OPEN ACCESS

Event attribution of a midlatitude windstorm using ensemble weather forecasts

To cite this article: Shirin Ermis *et al* 2024 *Environ. Res.: Climate* **3** 035001

ENVIRONMENTAL RESEARCH
CLIMATE

OPEN ACCESS

RECEIVED
7 November 2023

REVISED
10 April 2024

ACCEPTED FOR PUBLICATION
23 April 2024

PUBLISHED
15 May 2024

PAPER

Event attribution of a midlatitude windstorm using ensemble weather forecasts

Shirin Ermis[1,*], **Nicholas J Leach**[1,2], **Fraser C Lott**[3], **Sarah N Sparrow**[4] and **Antje Weisheimer**[5,6]

[1] Atmospheric, Oceanic, and Planetary Physics (AOPP), University of Oxford, Oxford, United Kingdom
[2] Climate X Ltd, London, United Kingdom
[3] Met Office Hadley Centre, Exeter, United Kingdom
[4] Oxford e-Research Centre, Engineering Science, University of Oxford, Oxford, United Kingdom
[5] National Centre for Atmospheric Science (NCAS), University of Oxford, Atmospheric, Oceanic and Planetary Physics (AOPP), Oxford, United Kingdom
[6] European Centre for Medium-Range Weather Forecasts (ECMWF), Reading, United Kingdom
[*] Author to whom any correspondence should be addressed.

E-mail: shirin.ermis@physics.ox.ac.uk

Keywords: extreme weather, midlatitude cyclones, extreme weather attribution, weather forecasting, storm Eunice, forecast-based attribution, storyline attribution

Supplementary material for this article is available online

Abstract

The widespread destruction incurred by midlatitude storms every year makes it an imperative to study how storms change with climate. The impact of climate change on midlatitude windstorms, however, is hard to evaluate due to the small signals in variables such as wind speed, as well as the high resolutions required to represent the dynamic processes in the storms. Here, we assess how storm Eunice, which hit the UK in February 2022, was impacted by anthropogenic climate change using the ECMWF ensemble prediction system. This system was demonstrably able to predict the storm, significantly increasing our confidence in its ability to model the key physical processes and their response to climate change. Using modified greenhouse gas concentrations and changed initial conditions for ocean temperatures, we create two counterfactual scenarios of storm Eunice in addition to the forecast for the current climate. We compare the intensity and severity of the storm between the pre-industrial, current, and future climates. Our results robustly indicate that Eunice has become more intense with climate change and similar storms will continue to intensify with further anthropogenic forcing. These results are consistent across forecast lead times, increasing our confidence in them. Analysis of storm composites shows that this process is caused by increased vorticity production through increased humidity in the warm conveyor belt of the storm. This is consistent with previous studies on extreme windstorms. Our approach of combining forecasts at different lead times for event attribution enables combining event specificity and a focus on dynamic changes with the assessment of changing risks from windstorms. Further work is needed to develop methods to adjust the initial conditions of the atmosphere for the use in attribution studies using weather forecasts but we show that this approach is viable for reliable and fast attribution systems.

1. Introduction

Extreme weather events are responsible for a large fraction of the economic and societal impacts of climate change (Leckebusch *et al* 2007, NOAA 2020, 2023). Stakeholders across society are exposed to risks from these events with profound implications for infrastructure, health, ecosystems, social and financial services. It is hence important to understand their mechanisms and the impact of anthropogenic climate change on extreme events.

Event attribution is a novel field in climate science developed over the past two decades (Allen 2003, Stott *et al* 2016, Otto 2017, Jézéquel *et al* 2018, Winsberg *et al* 2020). It aims to assess whether and how much specific extreme weather events have changed due to large-scale anthropogenic changes in climate. Most of the work in the field uses global circulation models (e.g. Stott *et al* 2004, Philip *et al* 2020, van Oldenborgh *et al* 2021). These global climate models were, however, not developed to represent weather accurately—they are typically used to assess large scale changes in climate such as global mean surface temperature or changes in large-scale circulation.

As a result, probabilistic attribution has mostly been used for large-scale weather events such as continental-scale heatwaves and droughts (Stott *et al* 2004, Dole *et al* 2011, Rahmstorf and Coumou 2011, Funk *et al* 2018, Schiermeier 2018, Kew *et al* 2021, Carbon Brief 2022). Events are more easily attributable if they are primarily thermodynamically driven because the models often misrepresent dynamic events and are highly uncertain on their trends with climate change (Woollings *et al* 2018, Oudar *et al* 2020). Additionally, for dynamic changes such as changes in precipitation and storms, weather and internal variability adds a substantial amount of noise and climate change signals are less pronounced (Shepherd 2016).

A pre-requisite to successful event attribution is that the event under consideration can be modelled correctly. Initialised forecasts provide an ideal tool for this as the verification of their predictions will tell us immediately how well (or not) the event was simulated. Recent studies (Hope *et al* 2015, 2016, 2019, Leach *et al* 2021, 2024) have hence turned to successful seasonal and medium-range weather forecasts for attribution studies. These simulations, unlike Earth system models, have predictive skill due to their initialisation and assessments of skill with observations. This provides specificity to study the anthropogenic changes in a single event to great detail. This is what is called a storyline approach to event attribution and is in contrast to the risk-based approach in which the changes in frequency and severity of the event are the focus of the analysis.

Extratropical cyclones (ETCs) are some of the most frequent severe weather events in the midlatitudes and have been studied extensively. Their response to climate change until now and in the future depends sensitively on region, reference period as well as the intensity of cyclones analysed (Ulbrich *et al* 2009). Laurila *et al* (2021) examined the trend in all ETCs in Northern Europe for the period of 1980–2019 and found a linear declining trend of −3.7 cyclones per decade, although this trend was not significant at the 95% level. Studies by Sickmöller *et al* (2000), McCabe *et al* (2001), Raible *et al* (2008)indicate a decrease in the frequency of ETC for the North Atlantic and North Pacific for the second half of the 20th century, although Raible *et al* (2008) record an intensification in extreme cyclones (as defined by the 90th percentile in geopotential height gradients). An increase in frequency for the region around Iceland was found by Bartholy *et al* (2006), Schneidereit *et al* (2006)for the second half of the 20th century. This is in line with findings for 1958–1998 by Pinto *et al* (2009) who showed an increasing frequency in extreme cyclones near the British Isles, while total cyclone numbers in the North Atlantic have decreased by 10%. By the end of the 21st century, Priestley and Catto (2022) show a subtle decline in overall ETC frequency of around 5% using models from the Coupled Model Intercomparison Project, Phase 6. For extreme ETCs (defined by the 90th percentile of peak vorticity) in the Atlantic, Priestley and Catto (2022) observe a frequency increase in the same simulations. Both of these trends are in line with the above cited studies on ongoing trends indicating a continuation of current trends in the future. For the Mediterranean, a high number of studies point towards a decrease in winter cyclone activity when comparing current and future simulations in climate models (Carnell and Senior 1998, Nissen *et al* 2014). The former also finds a general decrease in cyclone activity in the North Pacific and the North Atlantic in a climate change scenario that goes beyond 1990 (Carnell and Senior 1998).

Some studies over the past decade (Cohen *et al* 2014, Barnes and Screen 2015, Hoskins and Woollings 2015, Woollings *et al* 2023) have hypothesised that Arctic Amplification has or will weaken the midlatitude jet stream and increases the persistence of weather regimes. This provides a possible explanation for the decrease in ETC frequency since formation of cyclones is directly impacted by the baroclinicity in the midlatitudes (Catto *et al* 2019).

Despite this decrease in ETC frequency, once a cyclone forms, there are some indications that extreme ETCs increase further in intensity as discussed above. An increase in diabatic heating from more humid air is able to explain this possible trend. Baroclinic storms gain potential vorticity (PV) through latent heating in the warm sector of the cyclone. As the warm air rises, PV is gained especially on lower levels and connecting low-level vorticity with upper-level vorticity to form a so-called PV tower (Rossa *et al* 2000). In a warmer atmosphere with a higher moisture content, this process would cause more intense cyclones with anthropogenic climate change.

Above, we discussed mainly studies of trends in contemporary cyclones or of cyclones in long climate projections. Another approach to assessing climate change signals in the frequency and intensity of cyclones is through event attribution studies—comparing individual storms in counterfactual scenarios. Most of the literature on the attribution of cyclones examines the effects of climate change on tropical cyclones. Multiple studies have used the pseudo-global warming approach for regional climate modelling (Schär *et al* 1996) and adapted it to initialised hindcasts to simulate Atlantic hurricanes in a warmer climate (Patricola and Wehner 2018, Reed *et al* 2022, Wehner and Reed 2022). These works suggest that cyclones tend to track further northward and increase in intensity. Recently, studies have also attempted to attribute midlatitude windstorms using reanalyses. Ginesta *et al* (2022) select synoptically similar days to the event in question ('analogue') and compare the analogues selected over different time periods to assess how the event has changed over time. The case study conducted in this work suggests that the extreme windstorm Alex which affected the South of France in October 2020 became more intense with climate change.

Hawkins *et al* (2023) discuss using a reanalysis and manipulating the data assimilation to model an observed storm in a warmer climate. For this, they use the same atmospheric observations to assimilate but perturb the sea surface temperatures and sea ice concentrations. For the storm Ulysses which hit Ireland and the UK in February 1903, they find that in today's climate the areas affected by high wind speeds would have been larger and precipitation increased.

Storyline attribution for cyclones is necessarily balancing the similarity of the synoptic conditions in the model to those observed before the event and implementing the climate change signal in the initial conditions. This is also true for our study. We are able to analyse changes in storm Eunice in great detail, but statements about the general evolution of midlatitude storms with climate change are limited due to the initialisation which preserves the synoptic conditions before the occurrence of the storm. The question we are trying to answer is how a storm with the dynamics of Eunice was impacted by climate change and how impacts might change if the synoptic conditions before Eunice were to arise in the future.

Storm Eunice hit the UK as the second named storm in a cluster of three storms that affected the UK in the span of one week in February 2022. After Dudley had previously impacted Scotland and northern counties of England on 16 February, Eunice affected mostly the southwest of England and resulted in two rare red weather warning zones for wind on 18 February. Despite these 'danger to life' warnings, four people lost their lives in the storm. Schools and businesses were closed and infrastructure impacted with the port of Dover closed for several hours. Recorded wind gusts reached 36 metres per second at exposed coastal regions (Kendon 2022). Eunice, called Zeynep by European weather services, later impacted Belgium, the Netherlands, northern Germany as well as the southwestern Baltic sea. Recovery efforts after Eunice were hampered by the impacts of storm Franklin on 21 February, three days after Eunice. Previous studies found that preceding storms in a cluster can enhance baroclinicity for subsequent storms (Weijenborg and Spengler 2020, Marcheggiani and Spengler 2023), a mechanism that might have contributed to the intensity of Eunice.

Storms Dudley and Eunice were both named on the same day, 14 February 2022, despite the fact that Eunice at that point was not a distinguishable feature. It eventually formed southwest of the UK with a strong interaction with upper level winds in the jet stream. The cyclogenesis of Eunice was explosive with the storm deepening by 30 hPa over the course of 18 hours (Kendon 2022). Volonté *et al* (2023a) find evidence of the occurrence of sting jets in Eunice's cloud head which likely added to the severe wind impacts from the storm.

2. Methods and data

We use operational medium-range weather predictions from ECMWF's ensemble prediction system (IFS EPS CY47R3, ECMWF 2021b) which have proven skill of representing midlatitude cyclonic systems and Eunice in particular. The predictability of storm Eunice within this system is shown in the supplementary material, and for the Met Office Unified Model in Volonté *et al* (2023a, 2023b). We compare the operational forecast (curr) at lead times of 2, 4, and 8 days to a pre-industrial (pi) and increased CO_2 (fut) scenario. The two counterfactual experiments have adjusted ocean temperatures as well as CO_2 concentrations changed to 285 ppm, 421 ppm, and 625 ppm for pi, curr, and fut respectively. The atmosphere is not adjusted at the time of initialisation. This has implications for the results of our attribution study, especially given the relatively short lead times of our simulations which are discussed later. Here, we try to mitigate these uncertainties by using three initialisation dates and comparing the attribution results across these simulations.

The three experiments are equidistant in their global radiative forcing so that if the response of storm intensity was linear with radiative forcing, the response in experiments should be symmetric around curr. Comparing three experiments instead of just two enables us to prevent attributing chaotic responses as in some cases the perturbations in initial conditions might lead the event to become less severe. Only comparing e.g. pi to curr in such a case could lead to false conclusions. To further prevent this, we also conduct a dynamical analysis of changes in the storms.

Each simulation, three initialisation dates per experiment, contains 51 ensemble members, with initial condition perturbations using singular vectors (ECMWF 2021b). These singular vector perturbations are identical across the three experiments. The model is fully coupled with an ocean model (NEMO3.4.1, Madec, 2008) and a sea ice model (LIM2, Fichefet and Maqueda (1997)). The atmospheric model component has a horizontal resolution of approximately 18 km (T_{Co}639) with a model timestep of 12 min. There are 137 vertical model levels in the atmosphere.

We compare these simulations to ERA5 (Hersbach *et al* 2020) using the deterministic product at an atmospheric horizontal resolution of 0.25°, corresponding to roughly 31 km at the equator, and a model timestep of 12 min. As the forecast model, ERA5 has 137 vertical model levels. Results are also compared to the operationalised analysis (ECMWF 2021a) used to initialise the forecast model.

For the tracking of storms within forecasts and reanalysis, we use the Tempest Extremes algorithm (Ullrich and Zarzycki 2016, Zarzycki and Ullrich 2017, Ullrich *et al* 2021) which tracks local minima of sea level pressure with closed contours in a 6° radius. We also exclude candidate points with vorticities of less than 10^{-4} s. Eunice-like storms in the simulations were identified using three conditions.

(i) The first date of detection of the track must be within 12 hours of the time the track of storm Eunice was first detected in ERA5.
(ii) The location of first detection of the track must be within 10° of the detection of storm Eunice in ERA5. The distance is calculated as a quadratic sum of latitudinal and longitudinal distance in degrees.
(iii) The minimum mean sea-level pressure of the cyclone across the detected track must be less than 980 hPa.

Using these tracks, we can select spatial variables like vorticity fields and wind speeds around the cyclone centre in Lagrangian composites to compare storms independently of where they occur. For a fair comparison between storms in time, we select the time step at which each storm reaches its maximum deepening rate of the minimum pressure over a six-hour time step. The fields are then averaged across all tracked storms to analyse the dynamics and changes between forecast lead times and experiments. The data required to reproduce our results is made available online (Ermis and Leach 2024).

3. Results and discussion

The basis for our subsequent analysis and discussion of the storms in our experiments is that storm Eunice was well forecasted in the operational forecast issued by ECMWF. The stamp plots presented in the supplementary material for all initialisation dates and ensemble members demonstrate that even with an 8 day lead time to when the storm eventually hit the UK on 18 February 2022, strong wind gusts were forecasted although then still in the wrong regions and stronger than Eunice would be. The four-day lead time marks the day that the UK Met Office named the storm, two days before the storm centre emerged from the jet stream southwest off the coast of the British Isles. The forecasted storm then—while it still shows a northward bias in wind gusts—has comparable strength to the analysis in the most intense ensemble members. The intensity of the storm with two days lead time improves and at this time, the ensemble is also more homogeneous. We take these findings as a solid basis for our further analysis.

3.1. Intensity of the storm

We start by assessing changes in the intensity of the storms between our three experiments—pi, curr, and fut. To this goal, we calculate the local maximum wind gusts in time over the day storm Eunice hit the UK, 18 February 2022. This allows to account for different regions being exposed to strong winds at different times as well as different temporal evolutions in the ensemble members. We then calculate the 90th percentile of wind gusts across the 51 ensemble members and obtain one map of reasonable worst outcomes of the storms in each experiment and initialisation. For all initialisation dates except the shortest lead time, the simulations show a northward bias for the maximum intensity of the storm, caused by the strongest forecasted storms tracking further north than the mean of the ensemble. We assume this northward bias arises from the stronger storms typically tracking further north in the midlatitudes so that for the longer lead times the most intense wind gusts also occur further north. Putting this bias to the side and focussing on the intensity of the gusts, the strong wind gusts in the 8 day lead time simulation are further north in the pi (figure 1(a)) than in the curr (figure 1(b)). The fut experiment at 8 days lead time (figure 1(c)) shows stronger gusts forecasted for the South of the UK and northern France than in the curr while gusts are weaker in Ireland and the rest of the UK. In the simulation with 4 days lead time (figures 1(d)–(f)), the storms get more intense with additional forcing. We see a monotonic increase in the maximum gusts in the experiments as well as a clear increase in the area that is affected by high wind gusts. The shortest lead time simulations (figures 1(g)–(i)) all show very strong wind gusts that overestimate wind gusts in the gusts forecasted on the day the storm occurred (figure 1(j)) slightly. This is likely due to the smaller ensemble spread the closer we move towards the forecasted event which causes the 90th percentile of gusts to be more extreme at shorter lead times when

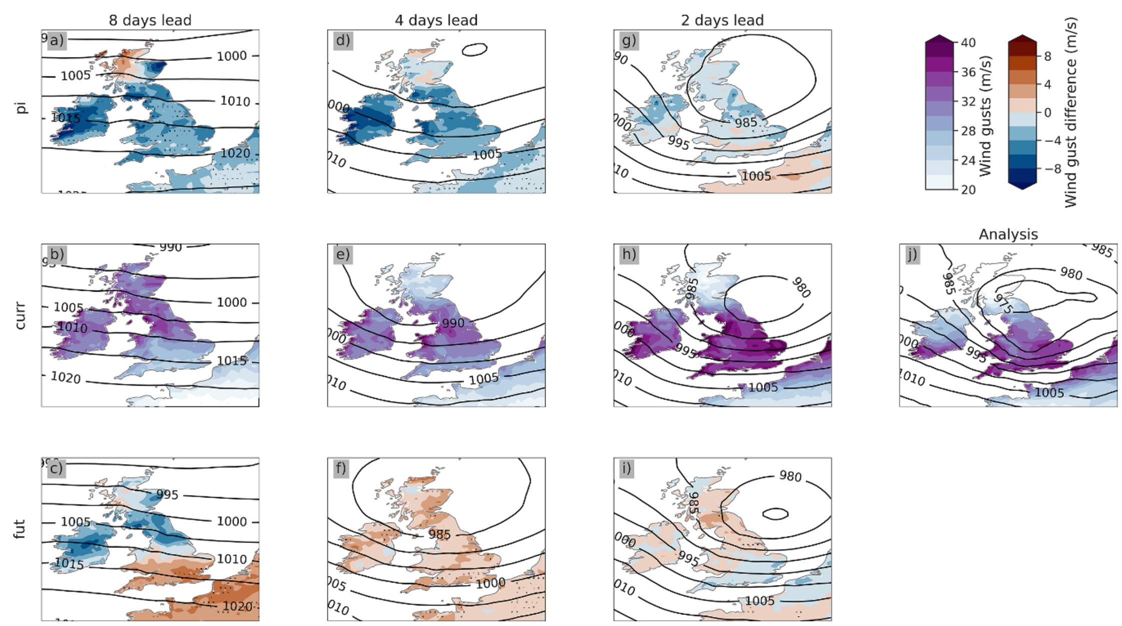

Figure 1. Changes in the local 90th percentile of wind gusts on 18 February 2022. Left three columns show the 90th percentile of wind across the ensemble after calculating the local maximum wind gust in time for each ensemble member. Panels for each of the three experiments (pi, curr, fut) and for the three initialisation dates as indicated. The panels for pi and fut show the difference in the wind gusts to the curr simulation at the same lead time, i.e. pi-curr in the top row and fut-curr in the bottom row. (a)–(c) pi, curr, and fut 90th percentile of wind gusts in the simulations with 8 days lead time to Eunice respectively, (d)–(f) same as before but for the 4 days lead time simulations, (g)–(i) same as before but for the 2 days lead time simulations. The fourth column (j) shows the same but in the forecast initialised at 00UTC on 18 February 2022. The pressure map in this panel is from the operational analysis at 12UTC on 18 February 2022, which is when Eunice hit the main of the UK. Black stippling shows areas where the difference between the counterfactuals and the curr is significant at the 90% level.

sufficiently conditioned on the storm. The intensity between the experiments at 2 days lead time is very similar, although the fut simulations (figure 1(i)) show a slightly stronger peak wind gusts in the northwest of the country.

We also calculate the footprint of the storms as defined by the area (over oceans and land) that is impacted by 10 metre gusts stronger than 20 metres per second at any time on 18 February. For the simulations at 4 days lead time, this footprint of the storm increases monotonically with climate forcing and is significant at the 90% level. The footprint is 11.54 million km^2 in the pi and 13.19 million km^2 in the fut simulation. Remaining footprints can be found in the supplementary material.

To quantify the aggregate impact of the storms more closely we use the storm severity index (SSI) as defined in Leckebusch *et al* (2008).

$$\mathrm{SSI}_{T,K} = \sum_{t}^{T}\sum_{k}^{K}\left[\left(\frac{\max\left(0, v_{k,t}\right)}{v_{\mathrm{Perc},k}} - 1\right)^{3} \times A_k\right], \tag{1}$$

where $v_{k,t}$ is the wind speed or gust in grid box k and at time t. A_k is the area of grid box k. $v_{\mathrm{Perc},k}$ is the percentile threshold of the wind speed or gust climatology at grid box k. For our analysis, we use the 98th percentile threshold in wind gusts. This threshold correlates well with the damage caused by a storm as local infrastructure is typically well adapted to the local wind climate (Leckebusch *et al* 2008). The original definition of the SSI uses wind speeds due to the then poor parameterisation in wind gusts (Leckebusch *et al* 2008). The parameterisation has since improved, and a comparison of the index using gusts and speeds showed little difference in the results. We decided to calculate the SSI using gusts here. Figure 2 shows the cumulative distribution of SSI in the 51 ensemble members for all three lead times and calculated for all land gridboxes over the UK and Ireland on 18 February 2022. At all lead times, the distributions are shifted towards more severe storms with climate change and this shift is statistically significant at the 8 and 4 day lead times ($p = 0.0003$ and $p = 0.000\,018$ respectively for a Kolmogorov–Smirnov (KS) test between the pi and fut simulations, figures 2(b) and (c)). We find that for the simulations at 8 days lead time (figure 2(a)), there are already significant differences between the curr and fut experiments, especially in the tail of the distributions where the fut simulations show especially strong SSI compared to the other two experiments. While this distance between the fut and the other two experiments decreases for the simulations at 4 days lead time (figure 2(b)), the three experiments are now all statistically different from each other as determined

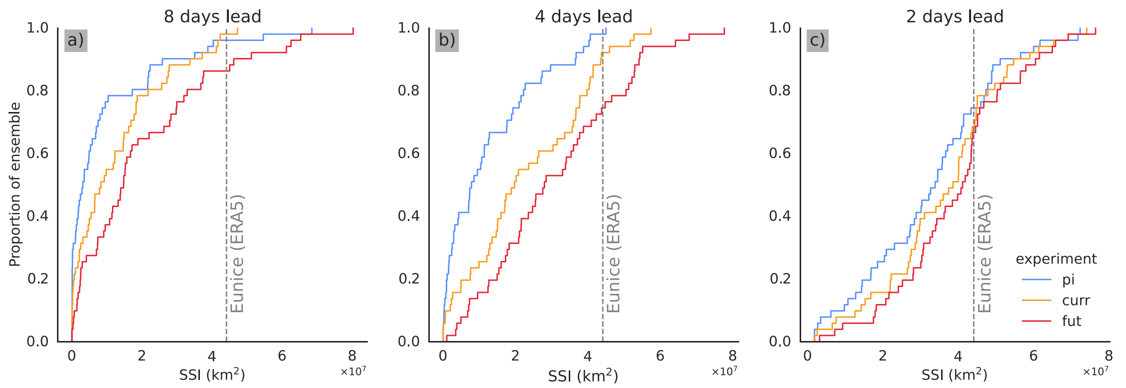

Figure 2. Empirical cumulative distribution functions of the SSI for the three experiments (pi, curr, fut) and the three initialisation times in separate panels. SSI is calculated using SSI and the definition from Leckebusch *et al* (2007) but using wind gusts instead of wind speeds. The SSI determined from ERA5 wind gusts is indicated by a dashed vertical line.

by a KS test. We theorise that this difference occurs due to higher variance in weather outcomes at longer lead times. Comparing the 2 days lead time simulations (figure 2(c)) does not result in statistically significant differences between the experiments. This is likely due to the strong conditioning on the storm at that lead time, and less atmospheric adjustment time which leads to a lower fraction of the total equilibrium response. This result fits in with the previous result from figure 1 that the maximum wind gusts at that lead time are very similar in the three experiments.

Using the SSI in figure 2, we can calculate the median increase in the storm's severity across the experiments. We calculate this increase for each ensemble member and then take the median across the ensemble. For the simulations with 4 days lead time (figure 2(b)), we obtain an increase in severity of a factor of 1.26 (90% confidence interval [0.37, 31.76]), or a 26% increase in severity, from pi to curr. We calculate a factor of 1.76 (90% confidence interval [0.82, 14.05]), or a 76% increase in severity, from curr to fut at the same lead time. These figures illustrate that, while not fully certain, it is very likely that extreme windstorms similar to Eunice will increase in their severity, potentially by a large degree.

The method for calculating the changes in the frequency of intense storms like Eunice is detailed in the supplementary material. This analysis compares the fraction of ensemble members reaching at least the SSI seen in ERA5 similar to the risk ratios calculated for traditional probabilistic attribution. Because we are using the storyline approach, we do not attribute the impact of climate change on the precursors already present in the initial conditions. Theoretically though, we would expect the risk ratio in long lead time simulations to asymptotically reach the threshold expected for an unconditioned simulation. This is, however, not the case for Eunice where the risk ratio at 8 days lead time is smaller than at 4. The risk ratios are 2.85 (90% confidence interval [2.49, 3.27]) and 1.72 (90% confidence interval [1.39, 2.13]) between the pi and fut experiments respectively for 4 and 8 days lead time. This could be due to the particular synoptic conditions 8 days prior to Eunice favouring a strong storm in the north of the UK more so than at 4 days lead time. While potentially an interesting method to combine storyline and probabilistic attribution, this risk ratio analysis does not yet yield conclusive results.

In the next step of our analysis, we use the tracked storms that satisfy the three conditions on track length, genesis region, and maximum depth of storm Eunice. We proceed with calculating a number of metrics on the tracks which are summarised in figure 3. There is good evidence that the minimum sea level pressure along the track reduces monotonically with increasing anthropogenic forcing (figure 3(a)). As expected from previous analyses, the 8 days lead time simulations are inconclusive due to large uncertainties. The 4 days lead time simulation shows a significant difference between the experiments pi and fut with deeper storms occurring in those simulations with stronger anthropogenic forcing. At 2 days lead time, the experiments maintain this ordering although the simulations are no longer significantly different from each other. In accordance with earlier results on the depth and gustiness of the storms with climate change, we also find that there is likely a trend towards a stronger peak vorticity (figure 3(b)) as well as 100 m wind speeds (figure 3(c)) with climate change. The maximum precipitation significantly increases at most lead times (figure 3(d)), indicating that a possible mechanism for intensification of the storm is through an increase in diabatic heating. In figure 3(e) we calculate the normalised deepening rate (NDR) of the detected storms as defined in Sanders and Gyakum (1980),

$$\mathrm{NDR} = \frac{\Delta p}{24\,\mathrm{hPa}} \frac{\sin(60^\circ)}{\sin(\Phi)}, \tag{2}$$

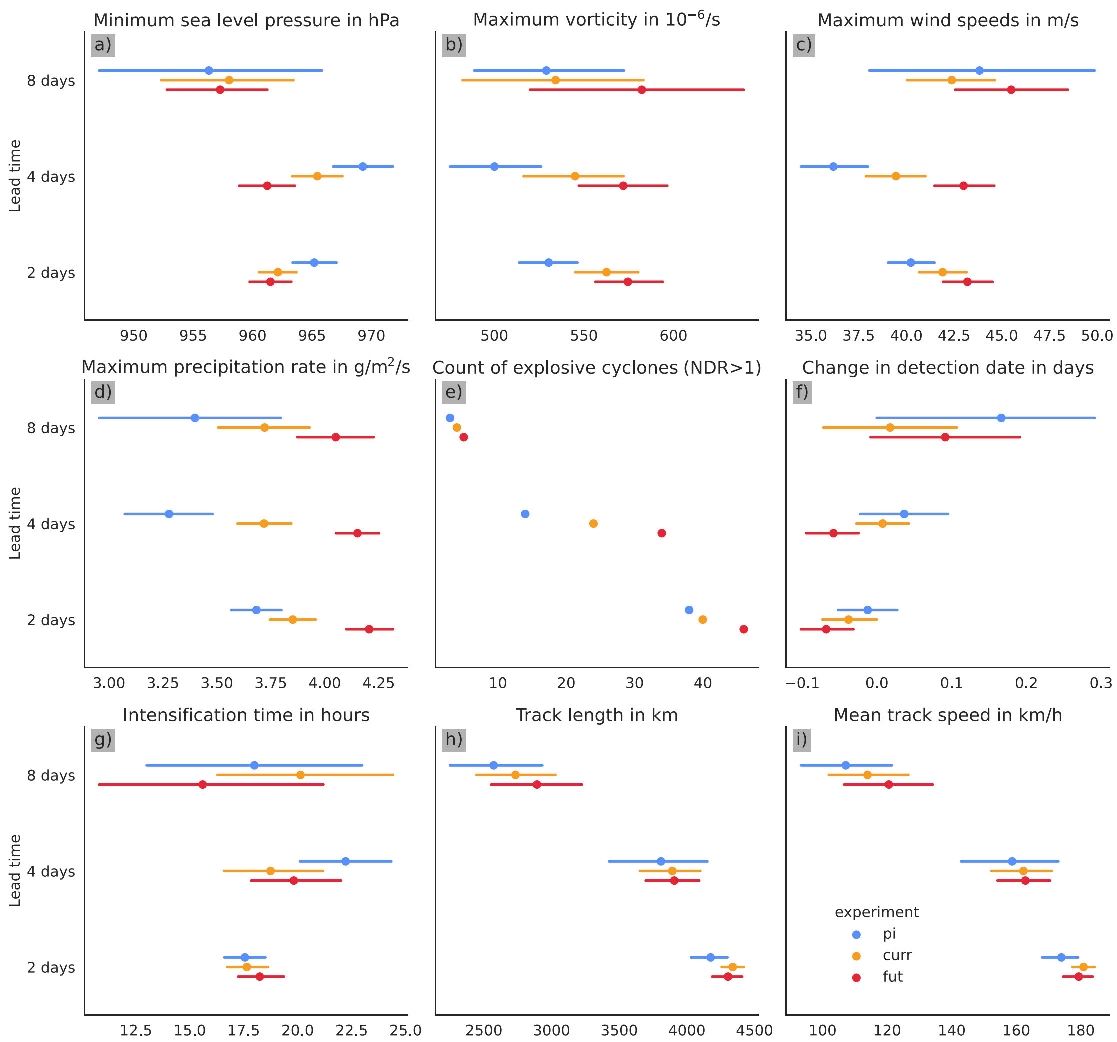

Figure 3. Summary metrics for all tracked storms with Eunice-like characteristics. Each panel highlights one metric as indicated. The colours refer to the three experiments (pi, curr, fut) and the ordinate indicates the three initialisation dates. (a) Minimum sea level pressure in the track (b) maximum vorticity along the track (c) maximum 100 m wind speed along the track within 10° latitude–longitude box of the cyclone centre (d) maximum precipitation in one three hour period along the track within 10° latitude-longitude box of the cyclone centre (e) count of storms with a normalised deepening rate (NDR) larger than one, i.e. number of explosive cyclones (f) change in onset date at which the track is first detected (g) deepening time of the storm defined as the number of hours from first detection to maximum vorticity (h) track length as detected by Tempest Extremes (i) Mean track speed between the times of maximum deepening and maximum vorticity. Confidence intervals are calculated by bootstrapping and for a 90% confidence interval.

where Δp is the maximum change in central pressure over a 24 hour period, and Φ is the latitude. Explosive cyclones are those storms that reach an NDR >1 which we count for each experiment and initialisation date. The number of explosive cyclones increases monotonically with climate change at all initialisation dates, with the largest changes at the 4 days lead time. For the onset date of the storms, i.e. the time at which the track is first detected using the tracking algorithm, we find that there is a trend towards an earlier onset date with climate change (figure 3(f)). The following panels of figure 3 highlight differences in track statistics of the intensification time, track length, time, and mean speed along the track. None of these statistics show significant changes with climate change that are consistent across lead times. We conclude that in our simulations in which the atmosphere is unchanged to the assimilated observations, the changes in the storms are limited to its intensity and cannot be tied to larger-scale track properties like the deepening time.

3.2. Dynamical analysis

Finally, we use the tracked Eunice-like storms for Lagrangian composites of the storms. The panels in figure 4 show the storms in each of the experiments averaged and in their own frame of reference and at 2 days lead time as this minimises the noise in the dynamical evolution of the storms. The main mechanism by which we expect the storms to intensify in the model is by diabatic heating. Indeed, comparing the specific humidity in the three experiments (or precipitation, see supplementary material), we find an increase in humidity at low

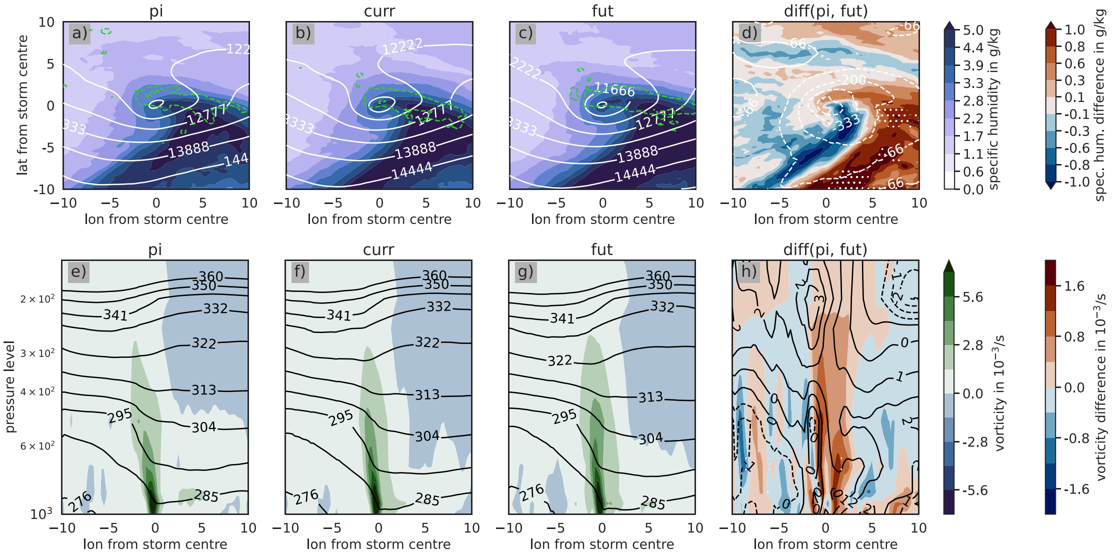

Figure 4. Storm composites of (a)–(d) 850 hPa specific humidity in shading and 850 hPa geopotential height in white contours (numbers indicate geopotential height values in metres). Green contours indicate upward vertical velocities of equal to or more than 0.5 m s^{-1}. (e)–(h) shows the East–West cross-sections of storms with vorticity in shading and potential temperatures in black contours. The plot shows the variables in the reference frame for all tracked storms at the maximum deepening of each storm by experiment. (a), (e) show storms in the pi simulation, (b), (f) the curr, (c), (g) the fut simulation, and (d), (h) shows the difference between storms in the fut and pi simulations. White stippling in the difference plots indicates confidence levels of 90% or over.

levels, especially in the region of the storm in which the warm conveyor belt is located. This goes beyond the general Northern Hemisphere increase in specific humidity and shows that the low-pressure system draws more moisture into the storm centre than the surrounding air. At the same time the cold sector of the storm shows a clear drying trend in a warmer atmosphere, possibly making dry intrusions and sting jets more intense. Figure 4 also shows the vertical vorticity tower in West-East cross-sections through the storm centres. As is typical for midlatitude cyclones, the centre of the storm shows a tower of vorticity that stretches from low levels to high up in the troposphere. The isentropes, shown as contours, show a clear slope between West and East highlighting the baroclinicity necessary for the development of a disturbance. We compare the cross-sections between the experiments and find that in the fut simulation, the central vorticity tower is increased in strength. This further supports our theory of stronger intensification through latent heating and subsequent vorticity production.

3.3. Discussion of limitations

As mentioned in the Methods section, using the same initial conditions in the atmosphere across the experiments has implications on the interpretation of results of this attribution study. The relatively short lead times in the simulations do not allow the atmosphere to adjust fully to the climate change forcing in the boundary conditions and ocean temperatures but only allows a fraction of the expected warming or cooling (in fut and pi, respectively). Leach *et al* (2021) discuss that the adjustment rate slows down the further we move away from the time of initialisation. We would hence expect the atmospheric temperature profile to have mostly adjusted to the forcing on the timescale of days (Tompkins and Craig 1998). Atmospheric circulation like the eddy-driven jet stream has longer adjustment timescales (Barry *et al* 2000) and is unlikely to have adjusted to the forcing in our simulations. Our study, however, explores the conditional case of how a storm similar to Eunice would have changed with climate change had it occurred in a different climate. Adjustments to the atmospheric circulation patterns are therefore less relevant as we are strongly conditioning on the synoptic conditions before the storm. We observe a consistent shift in the severity of the storm (figure 2) across the three different lead times. This indicates that independent of the level of atmospheric adjustment, the signal in the storm severity has the same sign. The local changes in wind gusts (figure 1) are less uniform across the lead times but here too, the monotonic shift across the three experiments in the two shorter lead times is a good indicator of a robust signal.

The shift in the maximum wind speeds across the tracked storms is highly significant and the dynamic analysis of tracked storms shows that an intensification has a physical basis in climate change. We hence conclude that despite a possible decreasing trend in the frequency of midlatitude cyclones, there are robust indications that Eunice and similar storms will become more intense in a warmer world when they do occur. The results are strictly only applicable to Eunice-like storms, but some of the physical changes we note may be more broadly applicable, though will depend on the specifics of each individual storm. In any case, understanding the rare and extreme cases is particularly important given their socioeconomic impacts.

4. Conclusion

In this work, we used initialised simulations with an operational forecast model to attribute changes in the extreme windstorm Eunice to climate change. This method was first introduced by Leach *et al* (2021) and has now been shown to work for dynamically-driven events such as midlatitude cyclones. Climate change signals in midlatitude cyclones, in particular their intensity in winds, are still uncertain due to their generally poor representation in coarse-resolution climate models. Our method of forecast-based attribution is able to determine the impact of climate change on a single storm, combining the forecast skill of well-resolved weather forecasts with the anthropogenic forcing of long-term climate simulations.

We produce two counterfactual scenarios in addition to the current-climate operational forecast: a pre-industrial and a future scenario to determine potential changes in storm Eunice which hit the UK in February 2022. We find that there is a monotonic increase in intensity in winds between the three climate scenarios. This is shown for maximum wind gusts across the UK and Ireland as well as for wind power by affected area (SSI). In tracked storms we find a decrease in the minimum sea level pressure as well as an increase in maximum vorticity, while other track statistics such as track speed and the deepening rate are not found to have a clear trend in our simulations. These results support previous findings (e.g. Ginesta *et al* 2022, Priestley and Catto 2022) that intense midlatitude cyclones are becoming stronger with climate change and highlight the importance of adaptation of infrastructure to intensifying winds.

Using composites of Eunice-like storms tracked using the Tempest Extremes algorithm, we propose that the mechanism by which Eunice intensifies with anthropogenic forcing is through increased specific humidity and latent heating in the warm conveyor belt where ascending air is producing vorticity through diabatic heating.

Atmospheric conditions are currently unchanged in the counterfactual simulations. This means that long-term circulation responses to climate change such as a weakened jet stream (Woollings *et al* 2023) are likely not represented in our simulations. However, given the strong conditioning on the synoptic situation before storm Eunice, we assume the effect of these signals to be small for this study. We explore this issue through the use of multiple initialisation dates but further work is needed to create realistic initial conditions for the atmosphere.

This work adds to existing attribution studies of storms (Lackmann 2015, Takayabu *et al* 2015, Ginesta *et al* 2022, Reed *et al* 2022) by introducing a method to reliably look at one specific event with well-defined climate forcings. Results are consistent with previous studies which found an increase in the intensity of winds in extreme midlatitude storms. Our study demonstrates that forecast-based attribution is a promising approach to studying the impact of climate change on dynamically driven events, which are typically more challenging to assess due to the current limitations of their representation within climate models.

Our results are important for a wide range of stakeholders in insurance, policy making, emergency management and adaptation planning. Although here we have examined a single high-impact event, and so results are not applicable to ETCs in general, the magnitude of some of the attributable changes we have found, suggests that it may be important to consider increasing wind design thresholds for future infrastructure developments.

Data availability statement

The data that support the findings of this study are openly available at the following URL/DOI: https://zenodo.org/records/10723245 (Ermis and Leach 2024).

Acknowledgments

S E was supported by the Natural Environment Research Council (NERC) under Grant NE/S0074747/1 and a Graduate Scholarship from St Cross College Oxford. N J L was supported by the Natural Environment Research Council under Grant NE/L002612/1 and the European Union's Horizon 2020 project FORCeS under Grant GA 821205. A W was supported by the NERC CANARI Project (NE/W004984/1) and by European Union's Horizon Europe research and innovation programme under Grant Agreement No. 101081460. F C L was supported by the Met Office Hadley Centre Climate Programme funded by the UK Department for Science, Innovation and Technology (DSIT). S N S was supported by the NERC Centre for Greening Finance and Investment (CGFI) under Grant NE/V017756/1. The results contain modified Copernicus Climate Change Service information [2022]. Neither the European Commission nor ECMWF is responsible for any use that may be made of the Copernicus information or data it contains. Acknowledgment is made for the use of ECMWF's computing and archive facilities in this research under the special project *spgbleac*. We thank two anonymous reviewers for their helpful comments on an earlier version of this paper.

ORCID iDs

Shirin Ermis https://orcid.org/0000-0002-3402-2633
Nicholas J Leach https://orcid.org/0000-0003-4470-1813
Fraser C Lott https://orcid.org/0000-0001-5184-4156
Sarah N Sparrow https://orcid.org/0000-0002-1802-6909
Antje Weisheimer https://orcid.org/0000-0002-7231-6974

References

Allen M 2003 Liability for climate change *Nature* **421** 891–2
Barnes E A and Screen J A 2015 The impact of Arctic warming on the midlatitude jet stream: can it? Has it? Will it? *WIREs Clim. Change* **6** 277–86
Barry L, Craig G C and Thuburn J 2000 A GCM investigation into the nature of baroclinic adjustment *J. Atmos. Sci.* **57** 1141–55
Bartholy J, Pongrácz R and Pattantyús-ábrahám M 2006 European cyclone track analysis based on ECMWF ERA-40 data sets *Int. J. Climatol.* **26** 1517–27
Carbon Brief 2022 (available at: https://www.carbonbrief.org/mapped-how-climate-change-affects-extreme-weather-around-the-world/#:~:text=Carbon%20Brief's%20analysis%20reveals%3A,events%20experienced%20some%20human%20impact.) (Accessed 3 November 2023)
Carnell R E and Senior C A 1998 Changes in mid-latitude variability due to increasing greenhouse gases and sulphate aerosols *Clim. Dyn.* **14** 369–83
Catto J L, Ackerley D, Booth J F, Champion A J, Colle B A, Pfahl S, Pinto J G, Quinting J F and Seiler C 2019 The future of midlatitude cyclones *Curr. Clim. Change Rep.* **5** 407–20
Cohen J *et al* 2014 Recent arctic amplification and extreme mid-latitude weather *Nat. Geosci.* **7** 627–37
Dole R, Hoerling M, Perlwitz J, Eischeid J, Pegion P, Zhang T, Quan X-W, Xu T and Murray D 2011 Was there a basis for anticipating the 2010 Russian heat wave?: the 2010 Russian heat wave *Geophys. Res. Lett.* **38**
ECMWF 2021a IFS Documentation CY47R3—Part II: data assimilation (available at: www.ecmwf.int/node/20196)
ECMWF 2021b IFS Documentation CY47R3—Part V ensemble prediction system (available at: www.ecmwf.int/node/20199)
Ermis S and Leach N 2024 Storm Eunice (February 2022): pre-industrial, current, and future climate scenarios using IFS EPS CY47R3 at 8, 4, and 2 days lead time [Data set] In *Environmental Research: Climate (1.0.0) Zenodo* (available at: https://doi.org/10.5281/zenodo.10723245)
Fichefet T and Maqueda M A M 1997 Sensitivity of a global sea ice model to the treatment of ice thermodynamics and dynamics *J. Geophys. Res.* **102** 12609–46
Funk C *et al* 2018 Examining the role of unusually warm Indo Pacific sea surface temperatures in recent African droughts *Q. J. R. Meteorol. Soc.* **144** 360–83
Ginesta M, Yiou P, Messori G and Faranda D 2022 A methodology for attributing severe extratropical cyclones to climate change based on reanalysis data: the case study of storm Alex 2020 *Clim. Dyn.* **61** 229–53
Hawkins E, Compo G P and Sardeshmukh P D 2023 ESD ideas: translating historical extreme weather events into a warmer world *Earth Syst. Dynam.* **14** 1081–4
Hersbach H *et al* 2020 The ERA5 global reanalysis *Q. J. R. Meteorol. Soc.* **146** 1999–2049
Hope P, Black M T, Lim E-P, Dowdy A, Wang G, Fawcett R J B and Pepler A S 2019 On determining the impact of increasing atmospheric CO_2 on the record fire weather in eastern australia in february 2017 *Bull. Am. Meteorol. Soc.* **100** S111–7
Hope P, Lim E-P, Wang G, Hendon H H and Arblaster J M 2015 Contributors to the record high temperatures across Australia in late spring 2014 *Bull. Am. Meteorol. Soc.* **96** S149–53
Hope P, Wang G, Lim E-P, Hendon H H and Arblaster J M 2016 What caused the record-breaking heat across Australia in october 2015? *Bull. Am. Meteorol. Soc.* **97** S122–6
Hoskins B and Woollings T 2015 Persistent extratropical regimes and climate extremes *Curr. Clim. Change Rep.* **1** 115–24
Jézéquel A, Yiou P and Radanovics S 2018 Role of circulation in European heatwaves using flow analogues *Clim. Dyn.* **50** 1145–59
Kendon M 2022 Storms Dudley, Eunice and Franklin *Technical Report* (Met Office National Climate Information Centre) (available at: www.metoffice.gov.uk/binaries/content/assets/metofficegovuk/pdf/weather/learn-about/uk-past-events/interesting/2022/2022_01_storms_dudley_eunice_franklin_r1.pdf)
Kew S F *et al* 2021 Impact of precipitation and increasing temperatures on drought trends in eastern Africa *Earth Syst. Dyn.* **12** 17–35
Lackmann G M 2015 Hurricane sandy before 1900 and after 2100 *Bull. Am. Meteorol. Soc.* **96** 547–60
Laurila T K, Gregow H, Cornér J and Sinclair V A 2021 Characteristics of extratropical cyclones and precursors to windstorms in northern Europe *Weather Clim. Dyn.* **2** 1111–30
Leach N J, Weisheimer A, Allen M R and Palmer T 2021 Forecast-based attribution of a winter heatwave within the limit of predictability *Proc. Natl Acad. Sci. USA* **118** e2112087118
Leach N, Roberts C, Aengenheyster M, Heathcote D, Mitchell D, Thompson V, Palmer T, Weisheimer A and Allen M 2024 Reliable heatwave attribution based on successful operational weather forecasts *Nat. Commun.* accepted
Leckebusch G C, Renggli D and Ulbrich U 2008 Development and application of an objective storm severity measure for the Northeast Atlantic region *Meteorol. Z.* **17** 575–87
Leckebusch G C, Ulbrich U, Fröhlich L and Pinto J G 2007 Property loss potentials for European midlatitude storms in a changing climate: loss potentials under climate change *Geophys. Res. Lett.* **34** L05703
Marcheggiani A and Spengler T 2023 Diabatic effects on the evolution of storm tracks *Weather Clim. Dyn.* **4** 927–42

McCabe G J, Clark M P and Serreze M C 2001 Trends in Northern Hemisphere surface cyclone frequency and intensity *J. Clim.* **14** 2763–8
Nissen K M, Leckebusch G C, Pinto J G and Ulbrich U 2014 Mediterranean cyclones and windstorms in a changing climate *Reg. Environ. Change* **14** 1873–90
NOAA 2020 (available at: https://www.noaa.gov/stories/record-number-of-billion-dollar-disasters-struck-us-in-2020) (Accessed 29 March 2023)
NOAA 2023 (available at: https://www.ncei.noaa.gov/access/billions/events.pdf) (Accessed 14 March 2023)
Otto F E 2017 Attribution of weather and climate events *Annu. Rev. Environ. Resour.* **42** 627–46
Oudar T, Cattiaux J and Douville H 2020 Drivers of the northern extratropical eddy driven jet change in CMIP5 and CMIP6 Models *Geophys. Res. Lett.* **47** e2019GL086695
Patricola C M and Wehner M F 2018 Anthropogenic influences on major tropical cyclone events *Nature* **563** 339–46
Philip S *et al* 2020 A protocol for probabilistic extreme event attribution analyses *Adv. Stat. Clim. Meteorol. Oceanogr.* **6** 177–203
Pinto J G, Zacharias S, Fink A H, Leckebusch G C and Ulbrich U 2009 Factors contributing to the development of extreme North Atlantic cyclones and their relationship with the NAO *Clim. Dyn.* **32** 711–37
Priestley M D K and Catto J L 2022 Future changes in the extratropical storm tracks and cyclone intensity, wind speed and structure *Weather Clim. Dyn.* **3** 337–60
Rahmstorf S and Coumou D 2011 Increase of extreme events in a warming world *Proc. Natl Acad. Sci. USA* **108** 17905–9
Raible C C, Della-Marta P M, Schwierz C, Wernli H and Blender R 2008 Northern Hemisphere extratropical cyclones: a comparison of detection and tracking methods and different reanalyses *Mon. Weather Rev.* **136** 880–97
Reed K A, Wehner M F and Zarzycki C M 2022 Attribution of 2020 hurricane season extreme rainfall to human-induced climate change *Nat. Commun.* **13** 1905
Rossa A M, Wernli H and Davies H C 2000 Growth and decay of an extra-tropical cyclone's PV-tower *Meteorol. Atmos. Phys.* **73** 139–56
Sanders F and Gyakum J R 1980 Synoptic-dynamic climatology of the "Bomb" *Mon. Weather Rev.* **108** 1589–606
Schär C, Frei C, Lüthi D and Davies H C 1996 Surrogate climate-change scenarios for regional climate models *Geophys. Res. Lett.* **23** 669–72
Schiermeier Q 2018 Droughts, heatwaves and floods: how to tell when climate change is to blame *Nature* **560** 20–22
Schneidereit A, Blender R, Fraedrich K and Lunkeit F 2006 Icelandic climate and north atlantic cyclones in ERA-40 reanalyses *Meteorol. Z.* **14** 16
Shepherd T G 2016 A common framework for approaches to extreme event attribution *Curr. Clim. Change Rep.* **2** 28–38
Sickmöller M, Blender R and Fraedrich K 2000 Observed winter cyclone tracks in the northern hemisphere in re-analysed ECMWF data *Q. J. R. Meteorol. Soc.* **126** 591–620
Stott P A *et al* 2016 Attribution of extreme weather and climate-related events *WIREs Clim. Change* **7** 23–41
Stott P A, Stone D A and Allen M R 2004 Human contribution to the European heatwave of 2003 *Nature* **432** 610–4
Takayabu I, Hibino K, Sasaki H, Shiogama H, Mori N, Shibutani Y and Takemi T 2015 Climate change effects on the worst-case storm surge: a case study of Typhoon Haiyan *Environ. Res. Lett.* **10** 064011
Tompkins A M and Craig G C 1998 Time scales of adjustment to radiative convective equilibrium in the tropical atmosphere *Q. J. R. Meteorol. Soc.* **124** 2693–713
Ulbrich U, Leckebusch G C and Pinto J G 2009 Extra-tropical cyclones in the present and future climate: a review *Theor. Appl. Climatol.* **96** 117–31
Ullrich P A and Zarzycki C M 2016 TempestExtremes v1.0: a framework for scale-insensitivepointwise feature tracking on unstructured grids *Clim. Earth Syst. Model.* **10** 1069–90
Ullrich P A, Zarzycki C M, McClenny E E, Pinheiro M C, Stansfield A M and Reed K A 2021 TempestExtremes v2.1: a community framework for feature detection, tracking and analysis in large datasets *Geosci. Model Dev.* **14** 5023–48
van Oldenborgh G J *et al* 2021 Pathways and pitfalls in extreme event attribution *Clim. Change* **166** 13
Volonté A, Gray S L, Clark P A, Martínez Alvarado O and Ackerley D 2023a Strong surface winds in Storm Eunice. Part 1: storm overview and indications of sting jet activity from observations and model data *Weather* **79** 40–45
Volonté A, Gray S L, Clark P A, Martínez Alvarado O and Ackerley D 2023b Strong surface winds in Storm Eunice. Part 2: airstream analysis *Weather* **79** 54–59
Wehner M F and Reed K A 2022 Operational extreme weather event attribution can quantify climate change loss and damages *PLoS Clim.* **1** e0000013
Weijenborg C and Spengler T 2020 Diabatic heating as a pathway for cyclone clustering encompassing the extreme storm dagmar *Geophys. Res. Lett.* **47** e2019GL085777
Winsberg E, Oreskes N and Lloyd E 2020 Severe weather event attribution: why values won't go away *Stud. History Phil. Sci.* A **84** 142–9
Woollings T, Barriopedro D, Methven J, Son S-W, Martius O, Harvey B, Sillmann J, Lupo A R and Seneviratne S 2018 Blocking and its response to climate change *Curr. Clim. Change Rep.* **4** 287–300
Woollings T, Drouard M, O'Reilly C H, Sexton D M H and McSweeney C 2023 Trends in the atmospheric jet streams are emerging in observations and could be linked to tropical warming *Commun. Earth Environ.* **4** 125
Zarzycki C M and Ullrich P A 2017 Assessing sensitivities in algorithmic detection of tropical cyclones in climate data *Geophys. Res. Lett.* **44** 1141–9